Velocity Fluctuations in Sedimenting Brownian Particles

Johannes Möller[†] and Theyencheri Narayanan[*]

ESRF—The European Synchrotron, 38043 Grenoble, France

We report a gradual transition of dynamics in sedimenting suspensions of charge stabilized Brownian particles prior to the onset of the macroscopic sedimentation front. Using multispeckle ultrasmall-angle x-ray photon correlation spectroscopy (USA-XPCS), we show that well-defined advective motions dominate the colloid dynamics during the early stages of sedimentation. With elapsing time, these advective currents decay and diffusive motions become the dominating contribution in the dynamics. Probing the temporal development of these fluctuations at smaller Peclet numbers (< 1) provides a new perspective for the mechanism determining the transient nature of velocity fluctuations in sedimentation and demonstrates new experimental capabilities enabled by multispeckle USA-XPCS.

Colloidal sedimentation is an extensively studied phenomenon, which for a long time has been identified as a powerful tool to probe the interactions and dynamics in particulate systems [1–4]. However, many aspects of the colloidal sedimentation are still the subject of extensive debate [5–8]. Especially at low Peclet numbers (Pe), where the Brownian motion dominates the particle dynamics, it is experimentally challenging to separate contributions from gravitationally induced advective and thermal diffusive motions. In a suspension with finite concentration, the hydrodynamic backflow causes a reduction of the sedimentation velocity from the Stokes velocity [2] and fluctuations in the particle number density leads to variance in the sedimentation speed [3–6].

Experimental studies of sedimentation on the particulate level have mainly been restricted to large non-Brownian particles due to practical constraints [9–11]. These investigations involved tracking a few tracer particles or particle imaging velocimetry (PIV) which provided mean sedimentation velocity, its variance and the velocity autocorrelation function. A striking result has been the suggestion that the long-range velocity fluctuations exhibit universal features [10,12]. This led to the proposal that sedimentation is analogous to high Rayleigh number and high Prandtl number turbulent convection [13]. However, later experimental and numerical studies have shown the transient nature of the velocity fluctuations and the dependence on the container size and particle concentrations [14–19]. Damping effects due to stratification have been proposed to govern the decay of velocity fluctuations [11,16,20]. In addition, it has been suggested that these scaling arguments may fail to explain very early parts of the time evolution [19]. Incomplete mixing also creates nonrandom particle distribution [6,21]. Numerical studies also indicate strong interplay between hydrodynamic and thermal fluctuations over a broad range of Pe [22].

In this Letter, we show that during the early stages of sedimentation, charge stabilized Brownian particles exhibit a similar advective behavior as previously found for non-Brownian suspensions [10]. To our knowledge, it is the first experimental observation of velocity fluctuations in sedimentation at low Pe range (< 1), where velocity and concentration fluctuations are decoupled. This provides a new insight on the microscopic origin of the temporal decay of velocity fluctuations, as macroscopic stratification and microscopic evolution of velocity fluctuations are separated to very different time scales at small Pe. The results demonstrate that the temporal decay of velocity fluctuations occur even before any macroscopic stratification effects are visible in the so-called column region. These velocity fluctuations may have implications in applications such as measurements of particle size and diffusion coefficients by dynamic light scattering (DLS) and in the analysis of near-field speckles generated by Brownian particles [23].

With PIV or DLS [10,16], it is challenging to obtain the full directional and length scale dependent dynamic information from small Brownian particles. Additionally, refractive index matching is necessary to prevent multiple light scattering. These limitations can be overcome by multispeckle ultrasmall-angle x-ray photon correlation spectroscopy (USA-XPCS), which is the x-ray analogue of DLS. The temporal fluctuations of scattered intensity provide access to the particle dynamics via the intensity-intensity autocorrelation function

$$g_2(\vec{q}, t) = \frac{\langle I(\vec{q}, \tau) I(\vec{q}, \tau + t) \rangle}{\langle I(\vec{q}) \rangle^2}, \tag{1}$$

where $\vec{q}$ is the scattering vector with magnitude, $q = 4\pi \sin(\theta/2)/\lambda$, λ is the wavelength (0.995 Å), and θ is the scattering angle. Experiments were performed at beam line ID02, ESRF, in a pinhole ultrasmall-angle x-ray scattering (USAXS) geometry [24]. This unique instrument allows XPCS measurements on aqueous particle suspensions down to the μm^{-1} q range [25]. Therefore, the same length and time
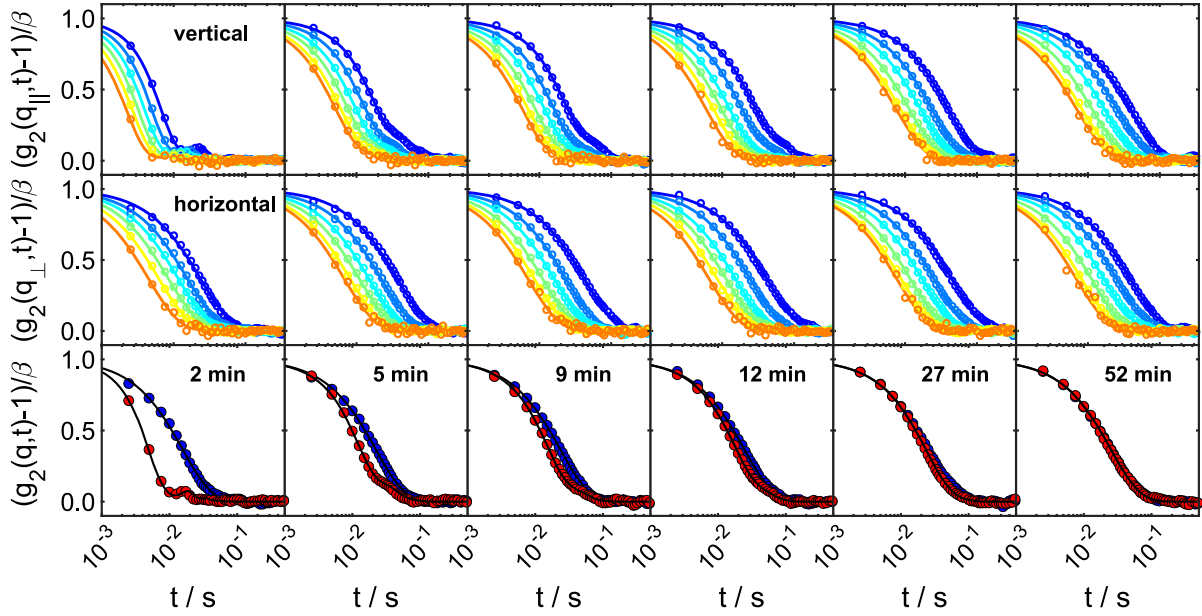
FIG. 1. Intensity autocorrelation functions measured in vertical (first row) and horizontal (second row) directions at different times after the sample was homogenized (2–52 min). The different colors correspond to q values of $q(\times 10^{-3}\ \text{nm}^{-1}) =$ 4.7 (dark blue) 6.3 (light blue) 7.7 (cyan) 9.3 (green) 10.7 (yellow) 12.3 (orange). In the third row, measurements in horizontal (blue) and vertical (red) directions are shown together for $q = 6.3 \times 10^{-3}\ \text{nm}^{-1}$.

scales as in DLS can be probed with a much smaller multiple scattering probability. Further details of the setup can be found in the Supplemental Material [26].

Charge stabilized silica spheres with a mean diameter of 590 nm ($\simeq$polydispersity 2%) dispersed in water were used for the measurements. Solutions were prepared at different particle concentrations from 0.5 to 15 vol % and contained in quartz capillaries of different sizes, in order to investigate the scaling of the velocity fluctuations with volume fraction and container dimension. The capillaries were filled up to a height of 47 mm and solutions were thoroughly mixed before the experiment. At first, XPCS measurements of a solution of 3.5 vol % silica spheres in a capillary with inner diameter of 1.1 mm will be discussed. The corresponding Pe is about 0.08.

The $g_2(\vec{q}, t)$ were measured as a function of height (z) above the bottom of the container (1, 5, 10, …, 45 mm) for different times after the homogenization of the sample. In Fig. 1 the first and second rows display the measured $g_2(\vec{q}, t)$ in the vertical, $g_2(q_\parallel, t)$ and horizontal, $g_2(q_\perp, t)$ directions, respectively, for $z = 30$ mm. The third row shows both directions for a single q value. The $g_2(q_\perp, t)$ over the whole course of the experiment can be described by a single exponential decay, corresponding to the diffusive behavior of particles perpendicular to the sedimentation direction. A more detailed discussion of the diffusive part and the related interparticle and hydrodynamic interactions is given in the Supplemental Material [26].

A strong deviation from diffusive behavior can be observed in the vertical direction right after the sample homogenization (2 min), as $g_2(q_\parallel, t)$ exhibits a periodic

modulation. This oscillatory feature is typical of directed motion of particles in a deterministic flow such as in uniform shear [31–33] or in laminar capillary flow [34,35]. The scattered intensity from a suspension of particles moving in a fluid is modulated by a frequency equals to the difference in Doppler shifts of all particle pairs in the scattering volume [36]. The advective motion of particles in the direction of the sedimentation gives rise to signature oscillations in $g_2(q_\parallel, t)$ which is consistent with elongated, swirl like velocity fluctuations previously observed in non-Brownian suspensions [10,12,20]. A probabilistic distribution of velocity, e.g., a Gaussian distribution, would not result in such oscillations but a monotonically decaying $g_2(q_\parallel, t)$ instead [36]. The resemblance of these structures to turbulent flow has been suggested before [12], but in that case the flow is isotropic which is clearly different from the anisotropic behavior of $g_2(\vec{q}, t)$ observed here.

The observed velocity fluctuations decay over the first hour of the experiment, corresponding to the oscillations shifting to longer times and smearing out. Then $g_2(q_\parallel, t)$ and $g_2(q_\perp, t)$ become identical. This implies a more randomization of the particle concentration by advective motion. In the picture of turbulence, this corresponds to velocity fluctuations not only slowing down but also decreasing in their overall extent, i.e., the break up of flow structure or eddies over time. This change of the dynamic behavior is in sharp contrast to the macroscopic behavior of the system, where the development and progress of a sedimentation front is on the time scale of several hours. In the following, we present a model that quantitatively describes the observed transition behavior.

Measured $g_2(\vec{q}, t)$ in both vertical and horizontal directions can be sufficiently described by including the diffusive and advective contributions to the particle dynamics [33],

$$|g_1(\vec{q}, t)|^2 = |g_{1,D}(q, t)|^2 |g_{1,v}(q_\parallel, t)|^2, \tag{2}$$

with $|g_{1,D}(q, t)|$ describing the diffusive and $|g_{1,v}(q_\parallel, t)|$ the advective parts of the dynamics, where $g_1(\vec{q}, t)$ and $g_2(\vec{q}, t)$ are connected via the Siegert relation. The measured $g_2(\vec{q}, t) = 1 + \beta |g_1(\vec{q}, t)|^2$, with β being the coherence factor of the experiment setup.

The temporal decay of the diffusive part of the particle dynamics is described by the well-known expression,

$$|g_{1,D}(q, t)|^2 = \exp[-2\Gamma(q)t]. \tag{3}$$

For noninteracting spheres, the relaxation rate is given by, $\Gamma = D_0 q^2$, with D_0 the free diffusion coefficient.

The second contribution depends on the velocity differences within the probed volume and can be calculated from a distribution of velocities, $N(\vec{v})$ [36],

$$
\begin{aligned}
|g_{1,v}(\vec{q}, t)|^2 = \int_0^\infty N(\vec{v_1}) \int_0^\infty N(\vec{v_2}) \\
\times \cos(\vec{q}t|\vec{v_2} - \vec{v_1}|) d\vec{v_1} d\vec{v_2}.
\end{aligned}
\tag{4}
$$

Because of the homodyne detection scheme, the mean sedimentation velocity does not influence $g_{1,v}(\vec{q}, t)$ and only velocity differences contribute. Therefore, the mean value of the distribution can be set to 0 without changing the calculated $g_{1,v}(\vec{q}, t)$. Furthermore, only velocities in vertical direction are considered. The resulting distribution function can be parametrized as

$$
N(v_\parallel) = \begin{cases} N_{\text{mean}}, & \text{for } 0 \le |v_\parallel| < \delta_v \\ N_{\text{fluc}}, & \text{for } \delta_v \le |v_\parallel| \le v_{\text{fluc}} + \delta_v \\ 0, & \text{for } v_{\text{fluc}} + \delta_v < |v_\parallel|, \end{cases}
\tag{5}
$$

with the first term representing particles narrowly distributed around the mean sedimentation velocity and the second, broader distribution accounts for velocity fluctuations. The maximum velocity difference due to fluctuations is $2v_{\text{fluc}}$ (with an infinitesimal small $\delta_v \to 0$), N_{mean} and N_{fluc} are numbers of particles within each of the two contributions. By normalizing the number distribution to 1, the ratio of fluctuating advective particles can be expressed as $\alpha = N_{\text{fluc}} v_{\text{fluc}}$. With this, $g_{1,v}(q_\parallel, t)$ follows as

$$|g_{1,v}(q_\parallel, t)|^2 = \left(1 - \alpha + \frac{\alpha}{q t v_{\text{fluc}}} \sin(q t v_{\text{fluc}})\right)^2. \tag{6}$$

Details of the calculation are provided in Supplemental Material [26]. When $\alpha = 1$, which corresponds to a uniform distribution of velocities, Eq. (6) becomes identical to
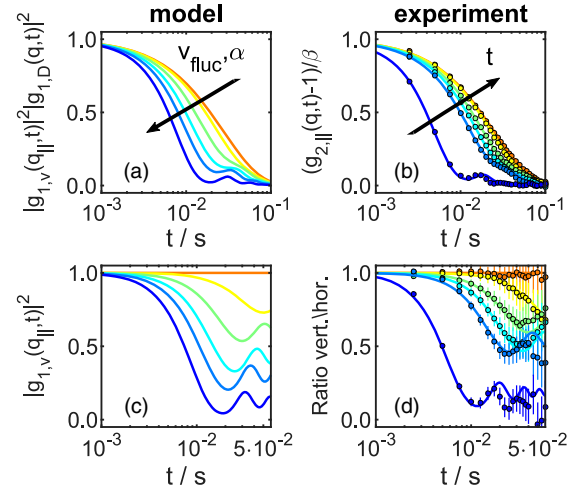
FIG. 2.   Comparison between the proposed model for velocity fluctuations and the measured XPCS $g_2(\vec{q}, t)$. Experimental data are shown for $q = 6.3 \times 10^{-3}$ nm^{-1}, measured within the first hour after sample homogenization. Corresponding plots for other q values can be found in the Supplemental Material [26]. Plots of expressions (2) and (6) are displayed in (a) and (c), respectively. Measurements in the vertical direction, and the ratio of vertical and horizontal signals, corresponding to $|g_{1,v}(q_\parallel, t)|^2$, are shown in (b) and (d), respectively. The fits were calculated by refining the model at all q values simultaneously.

the case of a constant shear flow previously described in Refs. [31–33]. The opposite case ($\alpha = 0$) corresponds to all particles having no vertical (or all the same mean) velocity. Therefore, $|g_{1,v}(q_\parallel, t)|^2 = 1$ and $g_1(\vec{q}, t)$ is determined by the diffusive contribution only.

A comparison of the derived model to the measured data is shown in Fig. 2. The observed time dependence of $g_{1,v}(q_\parallel, t)$ (b) can only be described by a simultaneous decrease of α and v_{fluc} (a), corresponding to a decrease of the population of fluctuating advective particles and absolute velocity differences, respectively. Furthermore, the ratio of the data in vertical and horizontal directions can be adequately described by the velocity fluctuation contribution $|g_{1,v}(q_\parallel, t)|^2$ [Figs. 2(c) and 2(d)], demonstrating that the diffusive and advective contributions in the model factorize very well.

The time dependence of the model parameters are shown in Fig. 3(a) at a height of $z = 30$ mm. The corresponding plots for $z = 10$, $z = 20$, and $z = 40$ mm are shown in the Supplemental Material [26], plots of v_{fluc} and α as a function of time and height are depicted in Figs. 3(b) and 3(c), respectively. The velocity fluctuations decay exponentially, which is in agreement with previous observation on non-Brownian particles [16]. Simultaneously, α decays corresponding to a fall in number of advective particles deviating from the mean velocity. This transformation occurs on a much shorter time scale than the macroscopic stratification observed by eye [Fig. 3(d)] and in the concentration
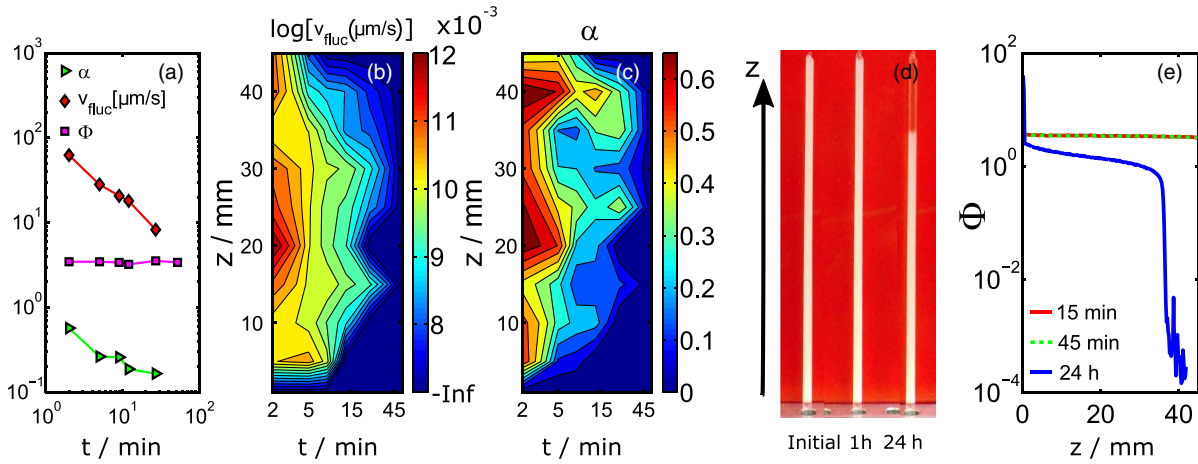
FIG. 3. (a) Time dependence of velocity fluctuations, v_{fluc}, α, and volume percent, ϕ for height, $z = 30$ mm. (b) Velocity fluctuations as a function of height and time. (c) α as a function of height and time. (d) Corresponding photographs of the solution taken at initial stage, 1 hour and 24 hours after onset of sedimentation. (e) Macroscopic stratification for different times after the onset of the sedimentation. Concentration profiles measured at 15 and 45 min superimpose.

calculated from the absolute SAXS intensities [Fig. 3(e)]. This finding supports the notion that stratification of the suspension is not the only parameter determining the initial decay of velocity fluctuations [19]. For small Pe, the stronger coupling between advective and Brownian motions may be driving the sharper decay of the velocity fluctuations.

An important feature of the velocity fluctuations is that the time decay of velocities can be described by an exponential master curve [16], $v_{\text{fluc}}(t) = v_0 \exp(-t/\tau)$, where v_0 and τ are the initial v_{fluc} and the characteristic decay time, respectively. To test this aspect at low Pe, we investigated different samples with varying container sizes and particle concentrations. The smallest container dimension was well above the limit of 140 times of particle radius, which was reported to show deviations from the universal scaling laws [16]. All the measured velocities show an exponential decay with time, as shown in Fig. 4. In (a), the initial concentration of the suspension was varied, the container diameter (0.9 mm) and the height ($z = 23$ mm) were fixed. Additionally, the container dimensions were varied at constant volume percent of 5% and 15%, the corresponding data are shown in the Supplemental Material [26]. It has been reported before, that the absolute value of the velocity fluctuations depends strongly on the experimental conditions such as the initial mixing [16,21]. We also cannot identify a discernible trend of the absolute value of velocity fluctuations as well as the characteristic decay time on the varied parameters. The obtained decay times are all in the range of 11–17 min. The most striking feature, however, is that all decays follow an exponential law when normalized by v_0 and τ which is displayed in Fig. 4(b). The same behavior was reported for velocity fluctuations in a non-Brownian system [16]. This observation suggests that velocity fluctuations exist in the Brownian regime, with the same characteristic decay behavior as a non-Brownian system. Furthermore, as the

measured characteristic decay times are far away from macroscopic stratification time scales, stratification effects cannot be the only reason for the nonuniversality of velocity fluctuations in sedimentation. In this case, the strong coupling with Brownian motion is likely promoting the sharper decay of velocity fluctuations and eventually dominating the dynamics. A similar behavior is observed when smaller particles (diameter 450 nm) are used. The fluctuation effect becomes less clearly discernible when the particle size is smaller and eventually superimposing with the faster diffusive part of the dynamics.

In summary, we used multispeckle USA-XPCS to probe velocity fluctuations in sedimentation at low Pe regime (<1). We observed well-defined advective motions manifested as oscillations in the measured $g_2(q, t)$, which can be quantitatively described by a simple model involving velocity fluctuations around a mean sedimentation velocity. These velocity fluctuations display similar exponential time decay
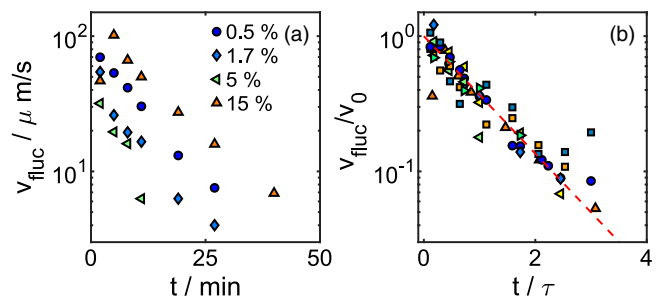
FIG. 4. (a) Time dependence of the velocity fluctuations for different particle concentrations, the container diameter (0.9 mm) and the height ($z = 23$ mm) are fixed. (b) Normalized velocity fluctuations for volume fractions between 0.005 and 0.15 and container dimensions between 0.2 and 2 mm. The corresponding unnormalized data are shown in (a) and Supplemental Material [26] [Figs. 5(a) and 5(b)].

as in a non-Brownian system reported before [16]. To our knowledge, this is the first experimental report of velocity fluctuations in a suspension of Brownian particles and it may help to address open questions in sedimentation dynamics. As compared to non-Brownian particles, the time scales of macroscopic sedimentation and decay of the microscopic velocity fluctuations are well separated in the system investigated here. This provides direct experimental evidence that the stratification is not the only parameter determining the decay of the velocity fluctuations. The stronger coupling between advective and diffusive motions may contribute to the gradual suppression of the velocity fluctuations at low Pe. In applications such as DLS and near-field scattering, velocity fluctuations might interfere with the determination of hydrodynamic radius and diffusion coefficients of particles susceptible to sedimentation. Since the measurement plane is horizontal in the conventional DLS setup, velocity fluctuation effects may go unnoticed without significant effect on the measured $g_2(q,t)$. However, this effect can be problematic in the analysis of near-field speckles and deriving dynamic information by that technique [37]. Furthermore, in the low Pe regime where diffusion and sedimentation velocity persist on similar time scales, the two contributions are usually difficult to separate experimentally. The presented study illustrates the advanced experimental capabilities enabled by multispeckle USA-XPCS to study the dynamical behavior of colloidal systems.

---

*Corresponding author.
narayan@esrf.fr
†Present address: European X-Ray Free-Electron Laser Facility, 22869 Schenefeld, Germany.

[1] J. Perrin, Ann. Chim. Phys. **18**, 5 (1909).
[2] G. K. Batchelor, J. Fluid Mech. **52**, 245 (1972).
[3] R. E. Caflisch and J. H. Luke, Phys. Fluids **28**, 759 (1985).
[4] E. J. Hinch, in *Disorder and Mixing*, edited by E. Guyon, J.-P. Nadal, and Y. Pomeau (Kluwer Academic, Dordrecht, 1988), Chap. IX, p. 153.
[5] S. Ramaswamy, Adv. Phys. **50**, 297 (2001).
[6] É. Guazzelli and J. Hinch, Annu. Rev. Fluid Mech. **43**, 97 (2011).
[7] R. Piazza, Rep. Prog. Phys. **77**, 056602 (2014).
[8] E. Lattuada, S. Buzzaccaro, and R. Piazza, Phys. Rev. Lett. **116**, 038301 (2016).
[9] H. Nicolai, B. Herzhaft, E. J. Hinch, L. Oger, and É. Guazzelli, Phys. Fluids **7**, 12 (1995).
[10] P. N. Segre, E. Herbolzheimer, and P. M. Chaikin, Phys. Rev. Lett. **79**, 2574 (1997).
[11] S.-Y. Tee, P. J. Mucha, M. P. Brenner, and D. A. Weitz, Phys. Fluids **19**, 113304 (2007).
[12] P. N. Segre, F. Liu, P. Umbanhowar, and D. A. Weitz, Nature (London) **409**, 594 (2001).
[13] P. Tong and B. J. Ackerson, Phys. Rev. E **58**, R6931 (1998).
[14] É. Guazzelli, Phys. Fluids **13**, 1537 (2001).
[15] A. J. C. Ladd, Phys. Rev. Lett. **88**, 048301 (2002).
[16] S.-Y. Tee, P. J. Mucha, L. Cipelletti, S. Manley, M. P. Brenner, P. N. Segre, and D. A. Weitz, Phys. Rev. Lett. **89**, 054501 (2002).
[17] L. Bergougnoux, S. Ghicini, É. Guazzelli, and J. Hinch, Phys. Fluids **15**, 1875 (2003).
[18] N.-Q. Nguyen and A. J. C. Ladd, J. Fluid Mech. **525**, 73 (2005).
[19] D. C. Gómez, L. Bergougnoux, J. Hinch, and É. Guazzelli, Phys. Fluids **19**, 098102 (2007).
[20] P. J. Mucha, S.-Y. Tee, D. A. Weitz, B. I. Shraiman, and M. P. Brenner, J. Fluid Mech. **501**, 71 (2004).
[21] L. Bergougnoux and É. Guazzelli, Phys. Fluids **21**, 091701 (2009).
[22] J. T. Padding and A. A. Louis, Phys. Rev. Lett. **93**, 220601 (2004).
[23] M. D. Alaimo, M. A. C. Potenza, M. Manfredda, G. Geloni, M. Sztucki, T. Narayanan, and M. Giglio, Phys. Rev. Lett. **103**, 194805 (2009).
[24] P. Van Vaerenbergh, J. Léonardon, M. Sztucki, P. Boesecke, J. Gorini, L. Claustre, F. Sever, J. Morse, and T. Narayanan, AIP Conf. Proc. **1741**, 030034 (2016).
[25] J. Möller, Y. Chushkin, S. Prevost, and T. Narayanan, J. Synchrotron Radiat. **23**, 929 (2016).
[26] See Supplemental Material at http://link.aps.org/supplemental/10.1103/PhysRevLett.118.198001 for details of the experimental setup, derivation of the model, and additional data, which includes Refs. [27–30].
[27] F. Westermeier, D. Pennicard, H. Hirsemann, U. H. Wagner, C. Rau, H. Graafsma, P. Schall, M. P. Lettinga, and B. Struth, Soft Matter **12**, 171 (2016).
[28] A. P. Philipse and A. Vrij, J. Chem. Phys. **88**, 6459 (1988).
[29] A. J. Banchio, J. Gapinski, A. Patkowski, W. Häußler, A. Fluerasu, S. Sacanna, P. Holmqvist, G. Meier, M. P. Lettinga, and G. Nägele, Phys. Rev. Lett. **96**, 138303 (2006).
[30] F. Westermeier, B. Fischer, W. Roseker, G. Grübel, G. Nägele, and M. Heinen, J. Chem. Phys. **137**, 114504 (2012).
[31] T. Narayanan, C. Cheung, P. Tong, W. I. Goldburg, and X.-l. Wu, Appl. Opt. **36**, 7639 (1997).
[32] W. R. Burghardt, M. Sikorski, A. R. Sandy, and S. Narayanan, Phys. Rev. E **85**, 021402 (2012).
[33] R. L. Leheny, M. C. Rogers, K. Chen, S. Narayanan, and J. L. Harden, Curr. Opin. Colloid Interface Sci. **20**, 261 (2015).
[34] S. Busch, T. H. Jensen, Y. Chushkin, and A. Fluerasu, Eur. Phys. J. E **26**, 55 (2008).
[35] A. Fluerasu, P. Kwasniewski, C. Caronna, F. Destremaut, J.-B. Salmon, and A. Madsen, New J. Phys. **12**, 035023 (2010).
[36] P. Tong, W. I. Goldburg, C. K. Chan, and A. Sirivat, Phys. Rev. A **37**, 2125 (1988).
[37] R. Cerbino, L. Peverini, M. Potenza, A. Robert, P. Bösecke, and M. Giglio, Nat. Phys. **4**, 238 (2008).